NWRI CONTRIBUTION 90-116

A NEW FACILITY FOR TESTING OF SUSPENDED SEDIMENT SAMPLER NOZZLES

by

Peter Engel

December 1989

MANAGEMENT PERSPECTIVE

Accurate measurement of suspended sediment concentration is important for application in a wide range of engineering and environmental problems. The Water Survey of Canada uses about 600 suspended sediment samplers in its national data collection program. Their calibration requires significant time and resources. Regular calibrations of the samplers are to be conducted in the towing tank at the National Water Research Institute in Burlington, Ontatio.

To facilitate the sampler calibrations, a static head test facility was developed to calibrate sampler nozzles for use with a particular type of sampler. In addition, the facility will be used to conduct development research on sampler calibrations. This report completes the first stage of the sampler calibration strategy presented by Engel and Zrymiak (1989).

Dr. J. Lawrence
Director
Research and Applications Branch

PERSPECTIVE DE GESTION

Dans le cas d'un grand évantail de question environnementales et d'ingénierie, il importe d'obtenir des mesures précises de concentration de sédiments en suspension. En vertu de son programme national de collecte des données, les responsables des Relevés hydrologiques du Canada utilisent environ 600 échantillonneurs de sédiments en suspension. L'étalonnage de ces échantillonneurs demande beaucoup de temps et de ressources. On procédera à l'étalonnage régulier des échantillonneurs dans le bassin de halage de l'Institut national de la recherche sur les eaux de Burlington (Ontario).

Afin de faciliter l'étalonnage des échantillonneurs, on a élaboré un dispositif d'essais de charge statique permettant d'étalonner les buselures utilisées dans un type défini d'échantillonneur. En outre, ce dispositif servira dans des recherches de développement sur l'étalonnage d'échantillonneurs. Le présent rapport complète la première étape de la stratégie d'étalonnage d'échantillonneurs présentée par Engel et Zrymiak (1989).

J. Lawrence
Directeur
Direction de la recherche et des applications.

SUMMARY

The method of calibrating suspended sediment sampler nozzles has been examined using theoretical and dimensional analysis and experimental measurements. Based on the results, a static head nozzles test facility was designed and built. The facility will be used to calibrate nozzles for suspended sediment samplers commissioned for field use, and to conduct tests on other pertinent factors which may affect the performance of sampler nozzles.

RÉSUMÉ

On a étudié la méthode d'étalonnage des buselures d'échantillonneurs de sédiments en suspension, en ayant recours à une analyse théorique et dimensionnelle, ainsi qu'à des mesures expérimentales. Les résultats ont permis de mettre au point un dispositif d'essais de charge statique. Ce dispositif servira à étalonner les buselures dans le cas des échantillonneurs de sédiments en suspension commandés pour le terrain, ainsi qu'à mener des essais sur d'autres éléments pertinents qui pourraient entraver le fonctionnement des buselures d'échantillonneurs.

TABLE OF CONTENTS

1.0 INTRODUCTION

The accuracy of all suspended sediment samplers must be checked regularly to ensure that reliable data are obtained. Samplers are tested in a towing tank with a particular set of nozzles as a total system. In addition to the properties of the sampler body itself, the sampler performance is sensitive to the geometric and thus the hydraulic characteristics of the nozzles. In practice, nozzles often get damaged causing changes in their hydraulic characteristics, thus requiring their replacement.

The nozzles can be calibrated seperately or the sampler can be adjusted to be compatible with a given nozzle (Engel and Zrymiak, 1989). The calibration of the sampler nozzles must have a high degree of repeatability and must cover the range of nozzle velocities encountered under normal sediment sampling conditions. For this purpose a new constant head test facility was constructed in the Hydraulics Laboratory of the National Water Research Institute (NWRI). This new facility will be used to maintain quality control of all nozzles used by the Water Survey of Canada (WSC) in their national sediment measuring program. The test facilty is part of a calibration plan presented by Engel and Zrymiak (1989) and was designed and fabricated by the Research and Applications Branch (RAB) of the NWRI in support of the Sediment Survey Section of the WSC at headquarters in Ottawa. The funds for the fabrication of the test facility were provided by the Sediment Survey Section.

2.0 METHOD OF TESTING SEDIMENT SAMPLERS

2.1 Preliminary Considerations

The suspended sediment samplers operate on the premise that the velocity of flow through the nozzle is equal to the velocity of the streamflow surrounding the nozzle. This is known as iso-kinetic sampling. Samplers are

tested to ensure that this condition is achieved within an acceptable margin of error. For the purpose of sediment sampling control, the nozzle velocity and the streamflow velocity are expressed as a ratio given by

$$K = V_N/V_S \qquad (1)$$

where K = the sampler coefficient, V_N = the velocity in the nozzle and V_S = the streamflow velocity. The aim of the sampler tests is to achieve a value of K sufficiently close to 1.

The value of K has direct implications on the accuracy of sampling suspended sediment. When $K > 1$ the sampler will undersample suspended sediment concentration, whereas when $K < 1$, the sampler will oversample as shown in Figure 1 (Beverage and Futrell, 1986). The error in sampling the sediment concentration has been shown to vary with particle size. When sediments are in the silt and clay size (i.e. particle diameter < .06 mm) the error in sampling is within 5% if the sampler coefficient is in the range $0.4 < K < 4.0$. In contrast to this, when the sediment is in the sand size range, the sampling accuracy is very dependent on the value of K. It can be seen in Figure 1, that for a grain size of 0.45 mm, values of K must be in the range $0.88 < K < 1.20$ in order to maintain a sediment concentration accuracy of 5%. At first glance it would appear that for sampling of suspended sediment in the clay to silt sizes, adjustment of the samplers is not so critical. However, one must keep in mind that the sediment particle size is a function of the flow velocity. It can be seen from Figure 1 that for velocities as low as 60 cm/s, sediments can be expected to be in the sand sizes for which errors in the measurement of sediment concentrations is strongly dependent on the value of K. Therefore, it is important to ensure that the sediment samplers are adjusted as close as possible to the ideal value of $K = 1.0$.

The value of K for a given sampler depends on both the characteristics of the sampler body itself and the characteristics of the nozzle. Samplers are tested in a towing tank over the range of velocities encountered in the field.

Tests by Beverage and Futrell (1986) have shown that results from tests in towing tanks are not significantly different from results of tests conducted in turbulent flows in flumes. For each towing velocity, a water sample is collected over the measured time interval required to fill the sample bottle about 3/4 full. Care is taken that the sampler is equipped with the appropriate size of nozzle for the selected towing velocity. Using the collected sample the velocity of the flow through the nozzle is computed and and values of K are determined. If all values of K are sufficiently close to 1.0, then the tests in the towing tank are considered to be successful. Alternatively, if values of K are either smaller or larger than desirable, then additional steps must be taken.

2.2 Method of Altering the Value of K

In order to improve the sampler performance, it is recognized that the value of K may be influenced by changes to either the sampler body itself, the nozzle or both. If $K < 1.0$, the sampler intake velocity must be increased and in most cases this can be achieved by making suitable modifications to the nozzle or the air exhaust passages in the sampler body. Experience has shown that the most effective way of increasing the nozzle velocity is to change the nozzle outlet geometry (Beverage and Futrell, 1986). Careful reaming and chamfereing of the nozzle outlet will reduce the energy losses to permit sufficient increase in the nozzle velocity, thereby increasing the value of K. In contrast to this, a value of $K > 1.0$ may be corrected by making adjustments to the sampler by reducing the size of the air exhaust tube or the exhaust port in the sampler body, thereby increasing the energy losses in the sampler. This method is not always successful. Benson (1981) reports instances where it has been impossible to make sufficient adjustments to obtain an acceptable value of

K. Under such circumstances a sediment sampler cannot be used.

Sampler testing in a towing tank is very time consuming and expensive. Therefore, once the initial value of K has been obtained, any changes to the nozzles should be evaluated and made by alternate means.

2.3 Calibration of the Nozzles

A review of WSC sampler calibration methods by Engel and Zrymiak (1989), showed that nozzles were calibrated separately using a static hydraulic head obtained with a constant head tank. In using such a static head method it must be recognized that the flow field at the nozzle entrance for the cases of streamflow and static head are different.

When the sampler is placed into the streamflow, the flow approaches the nozzle on a broad front. If $K = 1$, the streamflow will pass straight into the nozzle while any stream lines on either side of the nozzle intake will be deflected as shown in Figure 2(a). For this condition the trajectories of the sediment particles are parallel to the streamlines of the flow entering the nozzle. As a result the sampler collects the correct proportions of water and sediment particles. When $K < 1.0$, the velocity in the nozzle will be slower than the streamflow velocity and as a result, an area of stagnation will develop at the head of the nozzle as shown in Figure 2(b). In this case the stream lines of the approaching flow will be deflected ahead of the nozzle entrance. However, the sediment particles, because of their inertia, will tend to continue on their original path toward the nozzle entrance. As a result, for a given sampling time, the sampler will undersample the water volume but collect a larger proportion of sediment particles, resulting in oversampling of the sediment concentration. Finally, when $K > 1.0$, the velocity in the nozzle will be greater than that of the approaching flow and streamlines in the vicinity of the nozzle intake will converge toward the intake as shown in Figure 2(c). Once again the sediment particles will resist the sudden change in direction and the

increase in water flow through the nozzle will not be accompanied by a corresponding increase in sediment particles. As a result, in this case the sampler will undersample the sediment concentration. In contrast to this, when the nozzle is under a static head, the flow field around the nozzle intake is generated by the flow passing through the nozzle itself. Accordingly, water will be drawn toward the nozzle inlet in a manner represented schematically by the stream lines shown in Figure 3. Fortunately, the difference in the flow fields is only felt at the head of the nozzle. From the nozzle intake downstream, the flow dynamics are the same regardless of the external flow conditions. Therefore, as long as the geometry of the nozzle head is always the same, any alterations to the nozzles to improve the value of K can be made downstream of the inlet. This approach is in agreement with methods reported by Beverage and Futrell (1986) and Benson (1981). These observations confirm that the static head method may provide an efficient way of completing the sampler evaluation without the use of the towing tank.

3.0 BASIC PRINCIPLES OF THE STATIC HEAD METHOD

3.1 General Equation for Velocity Coefficient

It can be shown from energy considerations, with reference to the schematic layout in Figure 4, that without energy losses, the velocity of the flow passing through a nozzle is given by

$$V_t = \sqrt{2\ g\ (H + l)} \qquad (2)$$

where V_t = theoretical velocity of the flow through the nozzle, H = the depth of water above the nozzle entrance, l = the length of the nozzle and g = the acceleration due to gravity. The velocity V_t is known as the ideal velocity.

In reality, the nozzle flow velocity is always less than the ideal velocity and this may be expressed as

$$V_N = C_v \sqrt{2\ g\ (H + 1)} \qquad (3)$$

where V_N = the nozzle velocity and C_v = a velocity coefficient which is always less than 1.0 because of energy losses due to friction, flow contraction and expansion. As a result the velocity head due to the flow passing through the nozzle must be equal to the difference between the total static head on the nozzle and the energy losses expressed as energy head. This can be written mathematically as

$$\frac{V_N^2}{2g} = (H + 1) - h_L \qquad (4)$$

where h_L = the energy head loss due to friction , flow contractions and expansions due to the nozzle. The energy head loss can be written as

$$h_L = f\ \frac{1}{d_i}\ \frac{V_N^2}{2g} + K_1\ \frac{V_N^2}{2g} + K^2\ \frac{V_N^2}{2g} \qquad (5)$$

in which f = the Darcy - Weisbach friction factor, d_i = the internal diameter of the nozzle, K_1 = energy loss coefficient for flow contractions and K_2 = energy loss coefficient for flow expansions. Combining equations (4) and (5) and

solving for V_N results in

$$V_N = \sqrt{\frac{2g\ (H + l)}{[\ 1 + f\ \frac{l}{d_i} + K_1 + K_2\ ]}} \qquad (6)$$

If one now compares equation (3) and (6), one observes that the velocity coefficient C_v can be expressed as

$$C_v = \frac{1}{\sqrt{1 + f\ \frac{l}{d_i} + K_1 + K_2}} \qquad (7)$$

3.2 Friction Factor

The friction factor can be expressed in functional form as

$$f = \phi\ [\ \varepsilon,\ d_i,\ V_N,\ \rho,\ \nu,\ \sigma\ ] \qquad (8)$$

where ϕ denotes a function, ε = the height of the surface roughness of the flow boundary in the nozzle, ν = the kinematic viscosity of the fluid, ρ = the density of the fluid and σ = the surface tension of the fluid. Using dimensional analysis, equation (8) can be reduced to the following dimensionless form:

$$f = \phi_1 \left[\frac{\varepsilon}{d_i},\ \frac{V_N d_i}{\nu},\ \frac{\rho d_i V_N^2}{\sigma} \right] \qquad (9)$$

where ϕ_1 denotes another function. Troskolanski (1960) states that for conduits with $d_i < 1.25$ cm, surface tension of the fluid must be taken into account. The values of d_i for the sampler nozzles are 3.2 mm, 4.8 mm and 6.4 mm, all of which are significantly smaller than the minimum diameter given by Troskolanski (1960). However, velocities of flow through the nozzles vary from about 0.5 m/s to 3.0 m/s. The heads required to obtain such velocities are large enough to make surface tension effects negligibly small. Therefore, equation (9) can be reduced to the more familiar form

$$f = \phi_2 \left[\frac{\varepsilon}{d_i}, \frac{V_N d_i}{\nu} \right] \qquad (10)$$

where ϕ_2 denotes another function.

The solution to equation (10) is available in the practical form of the Moody Diagram given in Figure 5. From this diagram, values of the friction factor can be obtained for known values of the relative roughness and the Reynolds number. Data from Engel and Zrymiak (1989) show that over the practical range of nozzle velocities, Reynolds numbers vary from 5000 to 10,000. This range is indicated on the Moody Diagram in Figure 5. Examination of the curves in Figure 5 reveals that in this range of Reynolds numbers, flows through the nozzles are always in the smooth turbulent regime. As a result, considerable changes in the relative roughness of the nozzle flow boundary will result in very small changes in the friction factor f. This suggests that, variations in roughness of the nozzle flow passages will not have an adverse effect as long as the imperfections do not significantly affect the cross-sectional area of the flow. For the three sizes of brass nozzles used, values of ε/d_i vary from 0.0002 to 0.0004 for which values of f are not significantly different. Therefore, for the case of sampler nozzles, one may consider that f is a function of the Reynolds number only, varying from 0.038

when Re = 5000 to 0.031 when Re = 10,000. A similar result can be expected for plastic nozzles.

3.3 The Nozzle Energy Loss Coefficients

The energy loss coefficients K_1 and K_2 represent the entrance losses and the exit losses respectively. The entrance loss coefficient K_1 can be expected to be dependent on the entrance geometry and fluid properties. This can be expressed in functional form as

$$K = \phi_3 \, [V_N, \, r, \, d_i, \, d_o, \, \rho, \, \nu] \qquad (11)$$

where ϕ_3 denotes a function, r = the radius of curvature of the entrance lip, d_o = the outside diameter of the nozzle and all other variables have already been defined. Using dimensional analysis, equation (11) can be reduced to the form

$$K_1 = \phi_4 \left[\frac{r}{d_i}, \, \frac{d_o}{d_i}, \, \frac{V_N d_i}{\nu} \right] \qquad (12)$$

where ϕ_4 denotes another function. The sampler nozzle is similar to a re-entrant intake (Simon, 1986). Values of K_1 for the intake shape of the sampler are not available. However data from Miller (1978) indicates that for a sharp edged intakes at Reynolds numbers above 10,000, values of K_1 vary as shown in Figure 6. The curve shows that K_1 is strongly dependent on the wall thickness to inside diameter ratio t/d_i when this is less than about 0.08. When $t/d_i > 0.08$, K_1 is constant at about 0.5, indicating that wall thickness for

sediment sampler nozzles is not important. The value of K_1 can be reduced by bevelling the intake edge. This can also be seen in Figure 6, which gives values of K_1 for a bevel angle of 45 degrees. In this case the thickness of the nozzle wall is more important and K_1 varies significantly with t/d_i for values of $t/d_i < 0.2$. For sampler nozzles values of $t/d_i > 0.2$ and the effect on K_1 is only minor. These results show that some increase in the efficiency of intakes can be obtained by making modifications to the geometry of the intake. However, for the sediment samplers, values of Reynolds numbers are in the range from 5000 to 10,000 which are about one order of magnitude lower than the minimum Reynolds number for which the curves in Figure 6 are valid. Therefore, one can expect some dependency of K_1 on the Reynolds number in the operating range of the sampler nozzles, although the relationship is not known.

The energy loss coefficient for the nozzle outlet can be expressed in a general functional form as

$$K_2 = \phi_5 [V_N, di, \theta, d_o, \rho, \nu] \qquad (13)$$

where ϕ_5 denotes a function, θ = the angle of expansion of the nozzle outlet and the remaining variables have already been defined. Using dimensional analysis equation (13) can be reduced to the more meaningful dimensionless form

$$K_2 = \phi_6 \left[\theta, \frac{d_o}{d_i}, \frac{V_N d_i}{\nu} \right] \qquad (14)$$

where ϕ_6 denote another function. The relative nozzle wall thickness d_o/d_i is not expected to be important and can be removed from further consideration. Therefore, K_2 can be expressed in the final dimensionless form as

$$K_2 = \phi_7 \left[\theta, \frac{V_N d_i}{\nu} \right] \qquad (15)$$

where ϕ_7 denotes yet another function. The available information on nozzles discharging into air is very limited and deals primarily with fire hose nozzles. Miller (1978) suggests that the value of K_2 can be estimated from the relationship

$$K_2 = \left[\frac{d_i^2}{d_i^2 0\ C_d} \right]^2 \qquad (16)$$

where C_d = the discharge coefficient, d_{io} = the inside diameter at the outlet of the nozzle. When $\theta = 0$, then $d_i = d_{io}$ and K_2 depends only on the square of the inverse of the discharge coefficient. Increasing the values of θ means increasing the nozzle diameter gradually from d_i to d_{io} at the outlet end of the nozzle. It is clear from equation (16) that for a given value of C_d significant reductions in K_2 can be achieved by small increases in d_i. For example, assuming that $C_d = 0.9$ and the nozzle flow passage is gradually increased from a diameter of 4.8 mm to 5.0 mm at the outlet, then the value of K_2 is reduced from 1.23 to 1.04. Unfortunately, values of K_2 cannot be determined from equation (16) alone. In the range of Reynolds numbers applicable to sampler nozzles, one can expect that K_2 will also depend on the Reynolds number. This Reynolds number effect on K_2 is not known and must be determined from experiments.

In view of the possible dependence of both K_1 and K_2 on the Reynolds number, it is more convenient to combine the two energy loss coefficients into a single coefficient, say, K_T. This coefficient can then be expressed as

$$K_T = \phi_8 \left[\frac{r}{d_i}, \frac{d_o}{d_i}, \frac{V_N d_i}{\nu} \right] \qquad (17)$$

where ϕ_8 denotes a function. The degree to which the velocity through the nozzle can be increased depends on the reduction in K_T that can be achieved.

3.4 Behaviour of the Velocity Coefficient

Considering the total energy coefficient K_T, the velocity coefficient C_v in equation (7) can now be written as

$$C_v = \frac{1}{\sqrt{1 + f \frac{l}{d_i} + K_T}} \qquad (18)$$

In addition, given the functional relationship for K_T in equation (17) and the fact that for the sediment nozzles the friction factor f is a function only of the Reynolds number, the velocity coefficient C_v can be expressed in the more general functional form given by

$$C_v = \phi_9 \left[\frac{r}{d_i}, \frac{d_o}{d_i}, \phi, \frac{V d_i}{\nu} \right] \qquad (19)$$

where ϕ_9 denotes another function. Equation (19) states that for a given geometry, the velocity coefficient is a function only of the Reynolds number.

Values of C_v were plotted versus the Reynolds number for typical brass sampler nozzles having diameters of 3.2 mm, 4.8 mm and 6.4 mm, using existing data. The plot, given as Figure 7, reveals that there is only a mild dependence of C_v on the Reynolds number, which is less than expected. The reason for this can be attributed to the fact that the velocity coefficient is a function of the square root of the inverse of the sum of the energy losses. The value of C_v increases by about 3.4%, 4.0% and 1.6% over the operating range of the 3.2 mm, 4.8 mm and the 6.4 mm nozzles respectively. These variations are within the expected 5% accuracy of obtaining the value of K for the sampler tests in the towing tank. The results indicate that temperature effects, as they pertain to the fluid properties, are not important. However, the effect of temperature on the nozzles due to contraction and expansion is not known and needs to be determined. This consideration is important because there may be significant differences in temperature between the water in the testing laboratory and in the field.

The degree to which the value of C_v can be increased in order to increase the value of K for the sampler, must be determined by experiment. Such experiments can be conveniently conducted using a constant head facility.

4.0 DESIGN OF STATIC HEAD TEST FACILITY

4.1 General Design Considerations

The nozzle test facility was designed to meet the research requirements proposed by Engel and Zrymiak (1989). To meet these requirements, the facility was designed with an isolated, constant volume flow system, consisting of a

fluid reservoir, a constant head tank and the nozzle test chamber. The vertical position of the latter can be changed to vary the static head on the nozzles. The main features of the design are shown schematically in Figure 8.

4.2 The Nozzle Test Chamber

Consistent and repeatable testing of the sampler nozzles requires steady and uniform flow conditions in the nozzle test chamber. To accomplish this, a cylindrical test chamber, isolated from the constant head tank was chosen. The test chamber has an inside diameter of 40 cm (16 in.) and a height of 95 cm (37.5 in.). Flow from the constant head tank to the test chamber is passed through four 1.9 cm (3/4 in.) inside diameter hoses connected to the base of the chamber as shown in Figure 9 (a). The use of four hoses of the given size and the chosen location of connection with the test chamber ensures that the inflow velocities at the base of the test chamber are small. As a result there are no significant flow circulations set up.

Each test nozzle is fastened to a detachable mount which serves simultaneously as the outflow conduit as shown in Figure 9(b). The nozzle mount was fabricated from acrylic to permit observation of the flow as it leaves the nozzles. The nozzle is placed in the proper test location by passing the nozzle mount through the hole in the centre of the base of the test chamber and securing it at a predetermined elevation. The vertical, concentric alignment of the nozzle and the outflow conduit ensures that the flow through the nozzle will be uniformly distributed for all anticipated test conditions. Further, to ensure that there will be no adverse flow circulations when water levels in the test chamber are near the minimum, a circular baffle, concentric with the centreline of the nozzle, has been included in the design.

The water level in the test chamber is changed by vertical movement of the test chamber. To accomplish this, the test chamber is fastened into a

vertical traversing frame as shown in Figure 10. The traversing frame permits the test chamber to travel over a vertical distance of about 75 cm. The movement of the frame is accomplished with two synchronized, power driven screw jacks fastened to the top of the main frame of the test facility as shown in Figure 11. This drive system permits very precise positioning of the test chamber.

4.3 Constant Head Tank

During each test the water level in the test chamber is maintained at a constant and steady level because the water is supplied by the constant head tank. Water is pumped from the reservoir at the base of the test facilty using a low head, magnetic drive pump. The performance curve for the pump is given in Figure 12. The capacity of the pump exceeds the maximum discharge required for the nozzle tests.

The tank is partitioned into two parts by a weir plate, thus creating a constant head compartment on the upstream side of the weir plate and an overflow compartment on the downstream side. The water enters the constant head compartment from the pump through a diffuser which reduces undesirable turbulence set up by the inflow jet. As the water is pumped into the constant head tank, the water level rises until the crest elevation of the weir plate has been reached. Thereafter the water will begin to flow over the crest into the overflow compartment. The water level in the constant head compartment will continue to rise until the head required to pass the overflow over the weir plate has been reached. The overflow drains through a discharge pipe back into the pumping reservoir. The constant head compartment is connected to the nozzle test chamber by four 1.9 cm (3/4 in.) inside diameter hoses, described in Section 4.2, placed parallel to the weir plate as shown in Figure 13.

4.4 Stilling Well

Water levels in the nozzle test chamber are measured using a graduated scale, with a resolution of 0.5 mm, mounted on a 5 cm (2 in.) inside diameter stilling well as shown in Figure 14. The stilling well is mounted on the traversing frame of the test chamber and is connected to the water column in the test chamber with a 1 cm (3/8 in.) inside diameter plastic tube at the base inside the cylindrical baffle.

5.0 PRELIMINARY TESTS

Tests were conducted, using brass nozzles compatible with the DH48 suspended sediment sampler. These tests were intended to establish the variability in the determination of the velocity coefficients at different static heads over the operating range of the test facility.

5.1 Test Procedure

Each sediment sampler is equipped with three sizes of nozzles, having inside diameters of 3.2 mm (1/8 in.), 4.8 mm (3/16 in.) and 6.4 mm (1/4 in.), each size being applicable to a particular range of velocities. The three nozzles are shown in Figure 15.

Prior to testing, a nozzle was selected, its length measured and fastened to the nozzle mount which was then secured in the base of the test chamber as described in Section 4.2 and shown in Figure 16. The outflow end of the nozzle mount was then sealed with a rubber plug provided for this purpose and the pump was turned on. As the water entered the constant head tank, it flowed immediately through the plastic hoses into the test chamber. The water was allowed to rise in the test chamber until the mouth of the nozzle was covered by several millimeters of water. The pump was then turned off and the

stopper removed from the nozzle mount. The water drained through the nozzle mount into the reservoir until the water surface was level with the mouth of the nozzle. This water level was noted on the graduated scale along the stilling well and taken as the reference datum during the tests for this nozzle.

Once the preliminary procedures were completed, the rubber plug was replaced in the outflow end of the nozzle mount, the pump was turned on and the test chamber was positioned for the first test. Initially, as the water entered the constant head tank, all of the water flowed directly into the test chamber. As the water level in the test chamber rose, the difference in water elevation between the constant head tank and the test chamber decreased and the rate of increase in water level in the test chamber decreased. When the water level in the constant head tank and the test chamber were equal, all flow into the test chamber ceased and the total pumped flow was passed through the overflow compartment of the constant head tank into the reservoir. At this time the rubber plug was removed from the nozzle mount to allow flow to pass through the nozzle into the water reservoir. Once again the water levels underwent a change until the difference between the water surface elevations in the constant head tank and the test chamber were equal to the head required to supply the discharge passing through the nozzle. When this steady state was reached, the required measurements were made.

The following measurements were carried out: the water level elevation in the test chamber stilling well relative to the reference datum, the volume of water discharged through the nozzle and the time required to pass that volume of water. The volume of water was measured using a 1 litre graduated cylinder. For each value of static head, the discharge was measured by intercepting the outflow jet from the nozzle with the graduated cylinder and simultaneously starting the quartz crystal stop watch. When the cylinder was nearly full (ie: about 950 c.c.), it was quickly withdrawn and the stop watch simultaneously stopped. Care was taken that the volume of water was always near 950 c.c. to ensure that errors in its measurement as well as in the corresponding time were sufficiently small. Using these measurements the theoretical velocity and the

actual velocity of the flow passing through the nozzle were computed. Tests were conducted for each nozzle at about ten different heads from about 1 cm to 65 cm. For each value of the head, measurements of water levels, volume of discharge and time were made 10 times in order to obtain a sufficiently large set of data for statistical analysis. The test data are given in Tables 1 for the 3.2 mm nozzle, Table 2 for the 4.8 mm nozzle and Table 3 for the 6.4 mm nozzle.

5.2 Data Analysis

The data in Tables 1,2 and 3 were used to compute the ideal nozzle velocity according to equation (2) and the actual nozzle velocity by dividing the discharge Q by the cross sectional area of the nozzle flow passage. Using these velocities, the coefficient C_v was computed from equation (3) together with the corresponding Reynolds numbers. These results are given in Tables 4,5 and 6 for the 3.2 mm, 4.8 mm and the 6.4 mm nozzles respectively.

Any one of the 10 nozzle velocity samples of magnitude V_N used to compute the mean for each flow condition can be expected to lie within the range

$$V_N = \overline{V}_N \pm t_c \, S_v \qquad (20)$$

where V_N = the value of a single velocity sample measured, $\overline{V}_N$ = the mean of all the measured velocities at a given head, t_c = the confidence coefficient from Student's "t" distribution at nine dgrees of freedom (Spiegel, 1961) and S_v = the standard deviation about the mean velocity. Equation (20) can be made dimensionless by dividing both sides by the mean V_N. In addition, since the coefficient of variation, say, $C = S_v/V_N$, one obtains

$$\frac{V_N}{\overline{V}_N} = 1 \pm t_c C \qquad (21)$$

The product $t_c C$ in equation (21) represents the relative variability of the velocity samples and is expressed as

$$E_v = 100\ t_c C \qquad (22)$$

where E_v is the relative variability of the velocity samples in percent. Values of E_v at the 95% confidence level were computed and are given in Table 4,5 and 6 for the 3.2 mm, 4,8 mm and 6.4 mm nozzles, respectively.

Values of E_v are plotted as a function of the mean velocities for the three nozzles in Figure 17. The data show that values of E_v for each nozzle are at most only mildly dependent on the magnitude of the nozzle velocity. It can also be seen from Figure 17 that the variability tends to increase as the size of the nozzle increases. The reason for this is that the volume of water which is collected to determine the discharge through the nozzles increases with the diameter of the nozzles. Measurements were made with a graduated cylinder having a 1 litre capacity. As the discharge increases, the cylinder fills up more quickly, thus increasing the error in the measurement of the time required to collect the volume of water. Obviously, the variability can be reduced by increasing the volume of water and thereby increasing the length of measuring time. However, the variability with the present method is less than 0.3% and this is sufficiently small, so that no changes in the test method are required.

Values of the velocity coefficient C_v for each size of nozzle were plotted as a function of the Reynolds number in Figure 18. Smooth average curves, fitted by eye, were drawn through the plotted data to facilitate easier comparison of the characteristics of the three nozzles. The curves exhibit the same trend of mild dependence of C_v on the Reynolds number as the curves in Figure 7. However, for a given value of the Reynolds number, values of C_v in Figure 18 are always a little larger than those in Figure 7, eventhough both Figures represent nozzles of the same type. The reason for this is that each set of nozzles has been adjusted to match a particular sediment sampler in order to obtain a value of K within 10% of the sought after value of 1.0. This is further proof that very small changes to the nozzles can result in significant changes in their performance.

6.0 CONCLUSIONS

6.1 Each suspended sediment sampler must be tested to ensure that it operates iso-kinetically. If tests in the towing tank indicate that the performance of the sampler deviates from iso-kinetic behaviour by more than 5%, then adjustments must be made. Experience has shown that such adjustments can be made either to the sampler body itself, the nozzles or both, depending on the degree of adjustment required.

6.2 Adjustment to the sampler bodies can be made by changing the air exhaust conduit and the air exhaust port to increase or decrease the resistance to the air outflow as required. Adjustments to the nozzles can be made by decreasing the hydraulic resistance and thus increasing the discharge through the nozzle which in turn increases the flow velocity through the nozzle.

6.3 Analysis indicates that small changes in boundary roughness of the flow passage in the nozzles has virtually no effect on the friction factor for the nozzles. This is due to the fact that the flow through the

brass nozzles is in the smooth turbulent flow regime. For the Reynolds numbers in the operating range of the brass nozzles, the friction factor varies from 0.038 to 0.031. Similar results can be expected for plastic nozzles.

6.4 Evidence has been obtained to indicate that small changes in the nozzle outlet geometry will result in significant reduction in energy losses with resultant increase in discharge and flow velocity through the nozzles.

6.5 The coefficient of velocity was found to vary mildly with the Reynolds number. Therefore, temperature effects on the performance of the nozzles as far as fluid properties are concerned will be minor. However, effects of water temperature on the material nozzle properties such as shrinking and expansion need to be examined.

6.6 For a given Reynolds number, the coefficient of velocity was found to increase as the diameter of the nozzles decreased. These results were obtained with typical brass nozzles but can be expected to be similar for plastic nozzles.

6.7 Tests with the static head facility have shown that determinations of nozzle flow velocities have a variability of less than 0.3% at the 95% confidence level. Therefore, the static head facility will be satisfactory for the calibration of suspended sediment sampler nozzles.

ACKNOWLEDGEMENTS

The static head facility was fabricated by G. Voros and K. Davies. The nozzle tests were conducted by C. Bil and all photographs were provided by D. Doede. The writer is very grateful for their dedicated efforts on this project. The writer is indebted to P. Zrymiak of the Sediment Survey Section, Water Survey of Canada for his careful review of the manuscript.

REFERENCES

Benson, D.A. 1981. Personal communucation to Mr. Yvon Durette, WSC. Department of the Army, St. Paul District Corps of Engineers, St Paul, Minnesota.

Beverage, J.P. and Futrell, J.C. 1986. Comparison of Flume and Towing methods for Verifying the Calibration of a Suspended Sediment Sampler. Water Resources Investigation Report 86 - 4193, U.S.G.S.

Engel, P. and Zrymiak, P. 1989. Development of a Calibration Strategy for Suspended Sediment Samplers - Phase I. NWRI Contribution 89 - 121, National Water Research Institute, Canada Centre for Inland Waters, Burlington, Ontario.

Miller, D.S. 1978. Internal Flow Systems. BHRA Fluid Engineering Series, Vol.5.

Spiegel, M.S. 1961. Theory and Problems of Statistics, Schaum Outline, Schaum Publishing Company, New York.

Troskolanski, A.T. 1960. Hydrometry, Theory and Practice of Hydraulic Measurements, Pergamon Press, New York.

TABLE 1

Test Data for 3.2 mm Sampler Nozzle

E_o cm	E_H cm	(H + l) cm	Q c.c.	S_Q c.c.
20.50	32.90	22.90	12.88	0.043
	40.90	30.90	15.12	0.021
	48.90	38.90	17.11	0.034
	56.90	46.90	18.91	0.024
	64.90	54.90	20.54	0.029
	72.90	62.90	22.08	0.026
	80.90	70.90	23.57	0.027

E_o = water surface datum elevation

E_H = water surface elevation above nozzle

Q = mean discharge through nozzle

S_Q = standard deviation of discharge

TABLE 2

Test Data for 4.8 mm Sampler Nozzle

E_o cm	E_H cm	(H+1) cm	Q c.c.	S_Q c.c.
20.90	32.90	22.20	27.58	0.042
	40.90	30.20	32.35	0.070
	48.90	38.20	36.59	0.068
	56.90	46.20	40.13	0.063
	64.90	54.20	43.65	0.090
	72.90	62.20	46.94	0.090

E_o = water surface datum elevation

E_H = water surface elevation above nozzle

Q = mean discharge through nozzle

$_sQ$ = standard deviation of discharge

TABLE 3

Test Data for 6.4 mm Sampler Nozzle

E_o cm	E_H cm	(H+l) cm	Q c.c.	S_Q c.c.
20.85	34.35	23.90	46.41	0.161
	41.95	31.50	53.63	0.153
	50.30	39.85	60.73	0.150
	58.30	47.85	66.98	0.199
	66.20	55.75	72.30	0.231
	74.30	63.85	77.73	0.197

E_o = water surface datum elevation

E_H = water surface elevation above nozzle

Q = mean discharge through nozzle

S_Q = standard deviation of discharge

TABLE 4

Computed Parameters for 3.2 mm Sampler Nozzle

(H+l) cm	2g(H+l) m/s	$\overline{V}_N$ m/s	E_v %	C_v	$V_N d_i/\nu$ 10
22.90	2.120	1.624	0.152	0.766	5.16
30.90	2.462	1.908	0.107	0.775	6.06
38.90	2.763	2.158	0.148	0.781	6.85
46.90	3.033	2.387	0.102	0.787	7.58
54.90	3.282	2.592	0.111	0.790	8.23
62.90	3.513	2.787	0.091	0.793	8.85
70.90	3.730	2.974	0.086	0.797	9.44

$\overline{V}_N$ = mean nozzle velocity

E_v = 95% confidence limits of V_N as percent

C_v = velocity coefficient

TABLE 5

Computed Parameters for 4.8 mm Sampler Nozzle

(H+l) cm	2g(H+l) m/s	$\bar{V}_N$ m/s	E_v %	C_v	$V_N d_i/\nu$ 10
22.20	2.087	1.549	0.116	0.742	7.38
30.20	2.434	1.817	0.167	0.747	8.65
38.20	2.738	2.055	0.138	0.751	9.76
46.20	3.011	2.254	0.124	0.749	10.73
54.20	3.261	2.451	0.159	0.752	11.67
62.20	3.493	2.636	0.148	0.755	12.55

$\bar{V}_N$ = mean nozzle velocity

E_v = 95% confidence limits of V_N as percent

C_v = velocity coefficient

TABLE 6

Computed Parameters for 6.4 mm Sampler Nozzle

(H+l) cm	2g(H+l) m/s	$\overline{V}_N$ m/s	E_v %	C_v	$V_N d_i/\nu$ 10
23.90	2.165	1.469	0.261	0.680	9.33
31.50	2.486	1.700	0.215	0.684	10.80
39.85	2.796	1.925	0.186	0.688	12.22
47.85	3.064	2.123	0.223	0.693	13.48
55.75	3.307	2.291	0.241	0.692	14.55
63.85	3.539	2.463	0.191	0.696	15.64

$\overline{V}_N$ = mean nozzle velocity

E_v = 95% confidence limits of V_N as percent

C_v = velocity coefficient

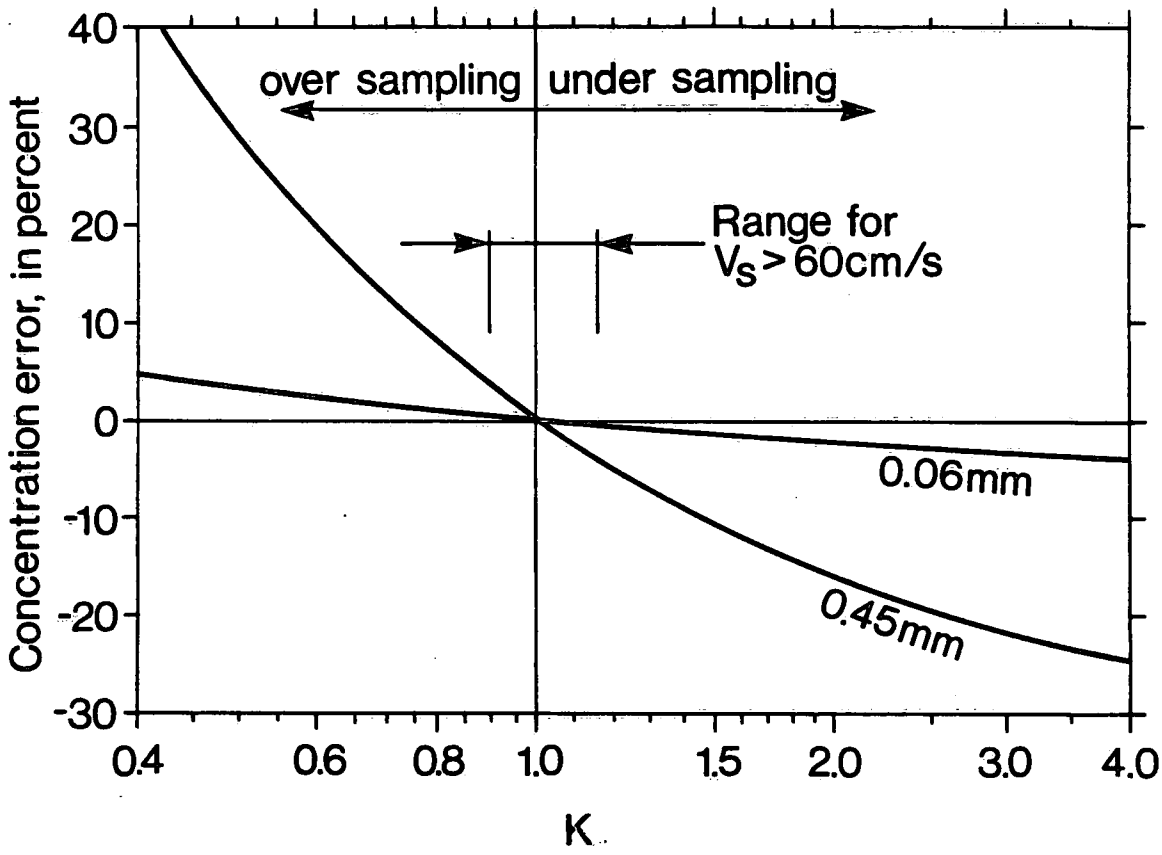

Figure 1 Effect of K and grain size on sampling error.

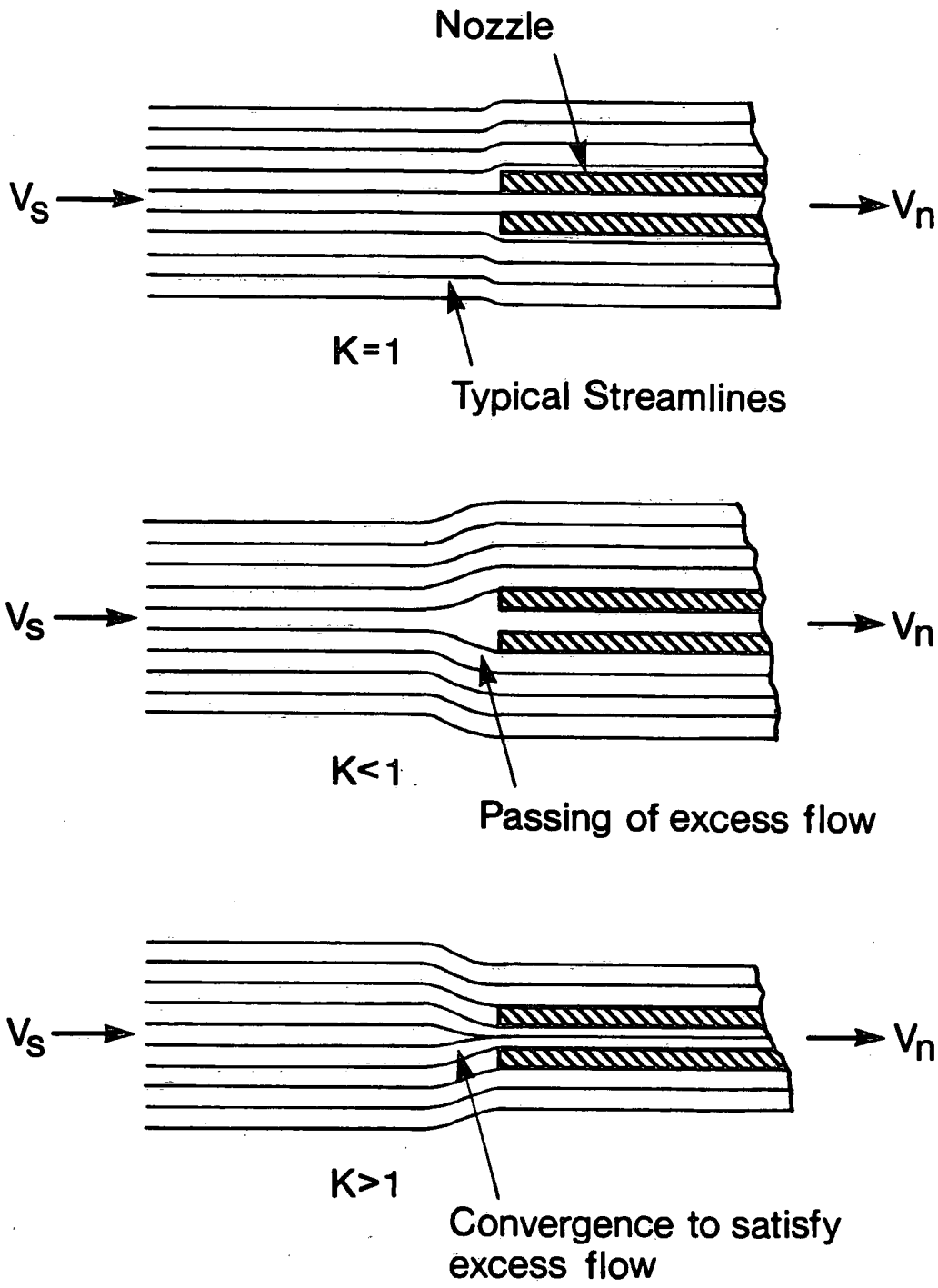

Figure 2 Flow pattern at nozzle nose for different values of K. in towing tank.

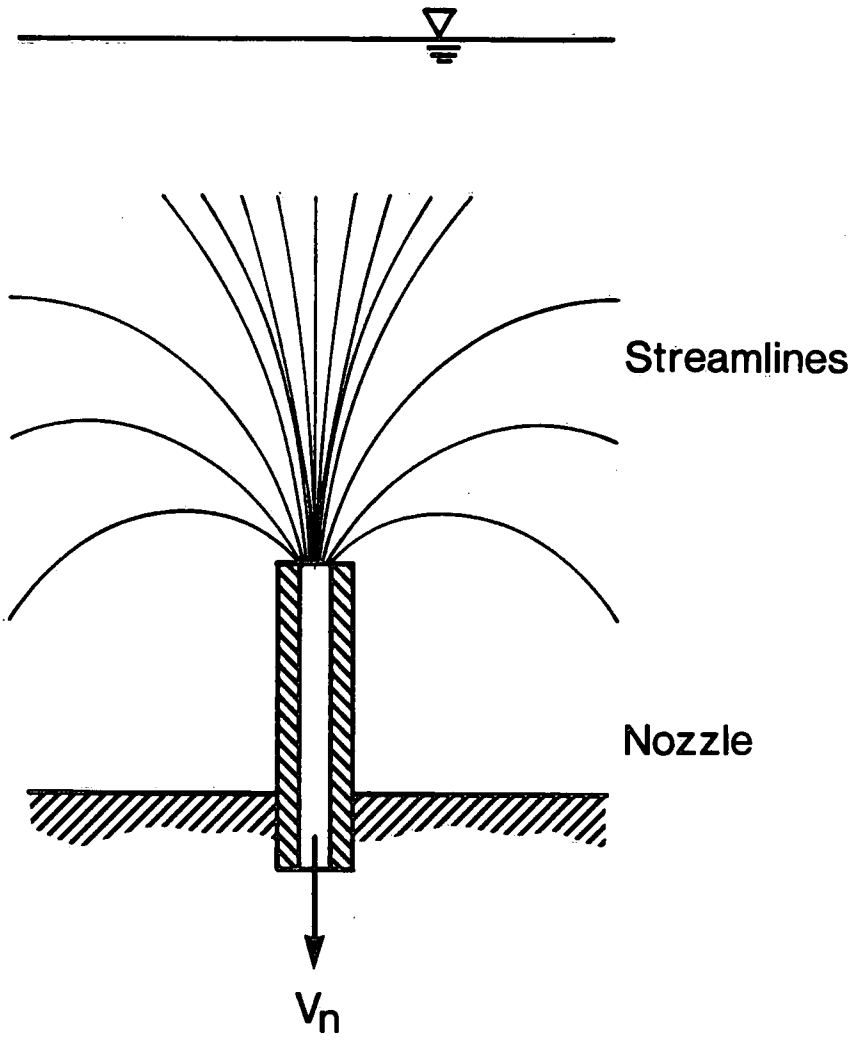

Figure 3 Flow pattern at nozzle nose under static head conditions.

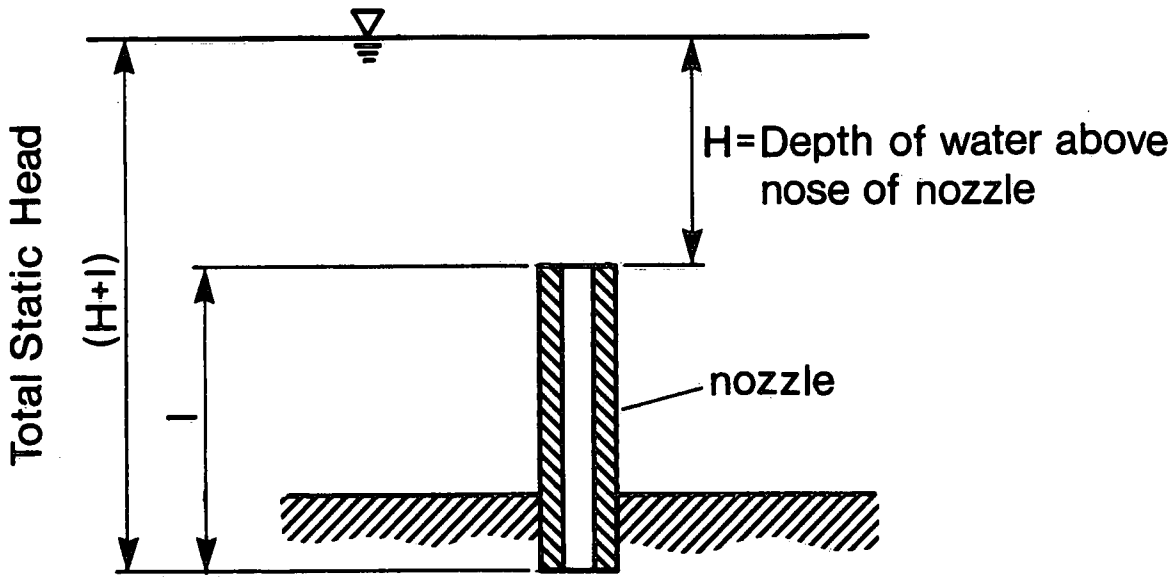

Figure 4 Static head on nozzle

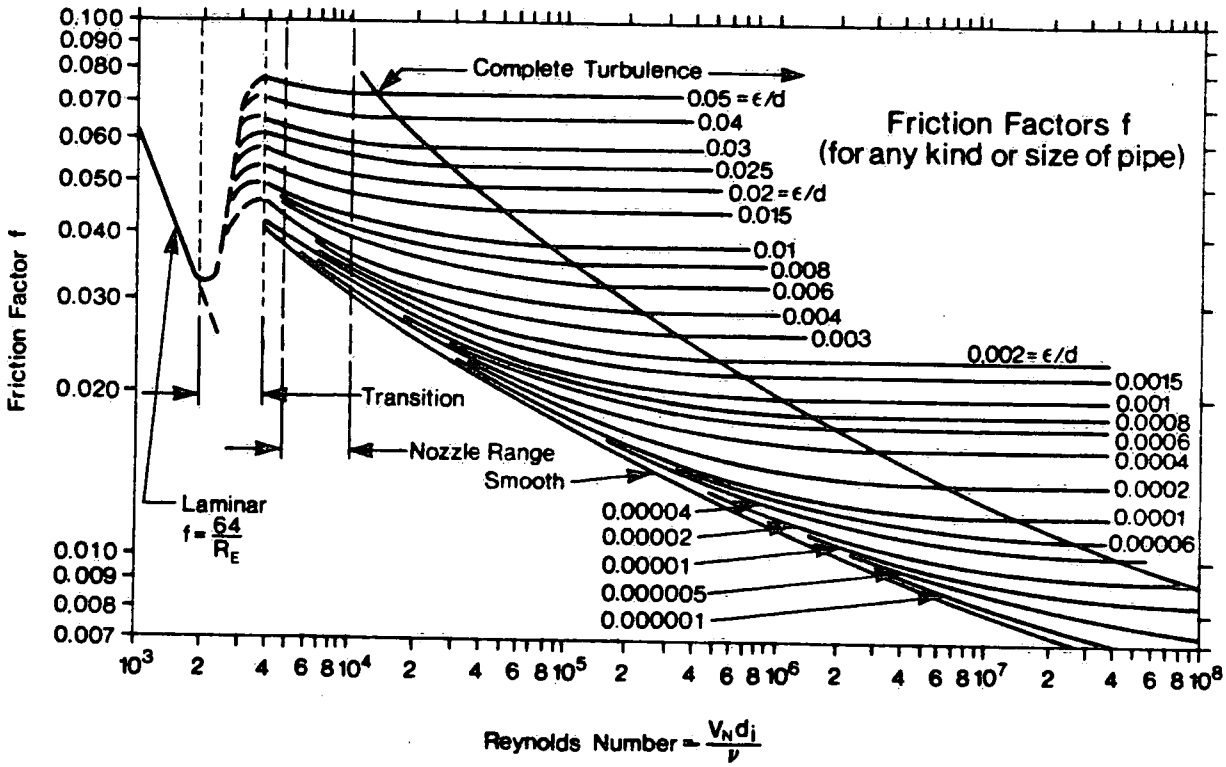

Kind of Pipe or Lining (New)	Values of ϵ in ft	
	Range	Design Value
Brass	0.000005	0.000005
Copper	0.000005	0.000005
Concrete	0.001 - 0.01	0.004
Cast Iron - uncoated	0.0004-0.002	0.0008
" " - asphalt dipped	0.0002-0.0006	0.0004
" " - cement lined	0.000008	0.000008
" " - bituminous lined	0.000008	0.000008

Figure 5 Moody Diagram

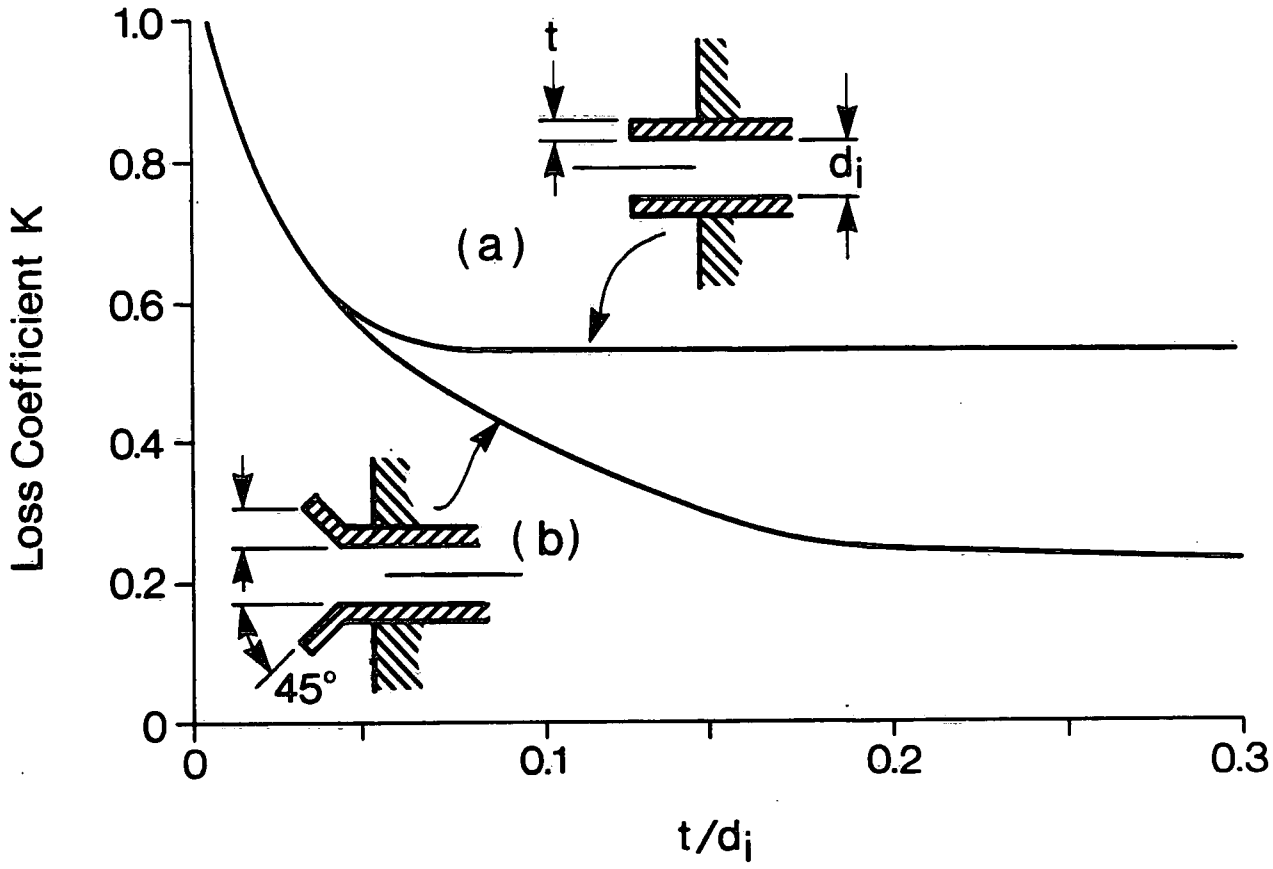

Figure 6 Variation of K for $\frac{V_N d_i}{\nu} > 10^4$ from (Miller, 1978)

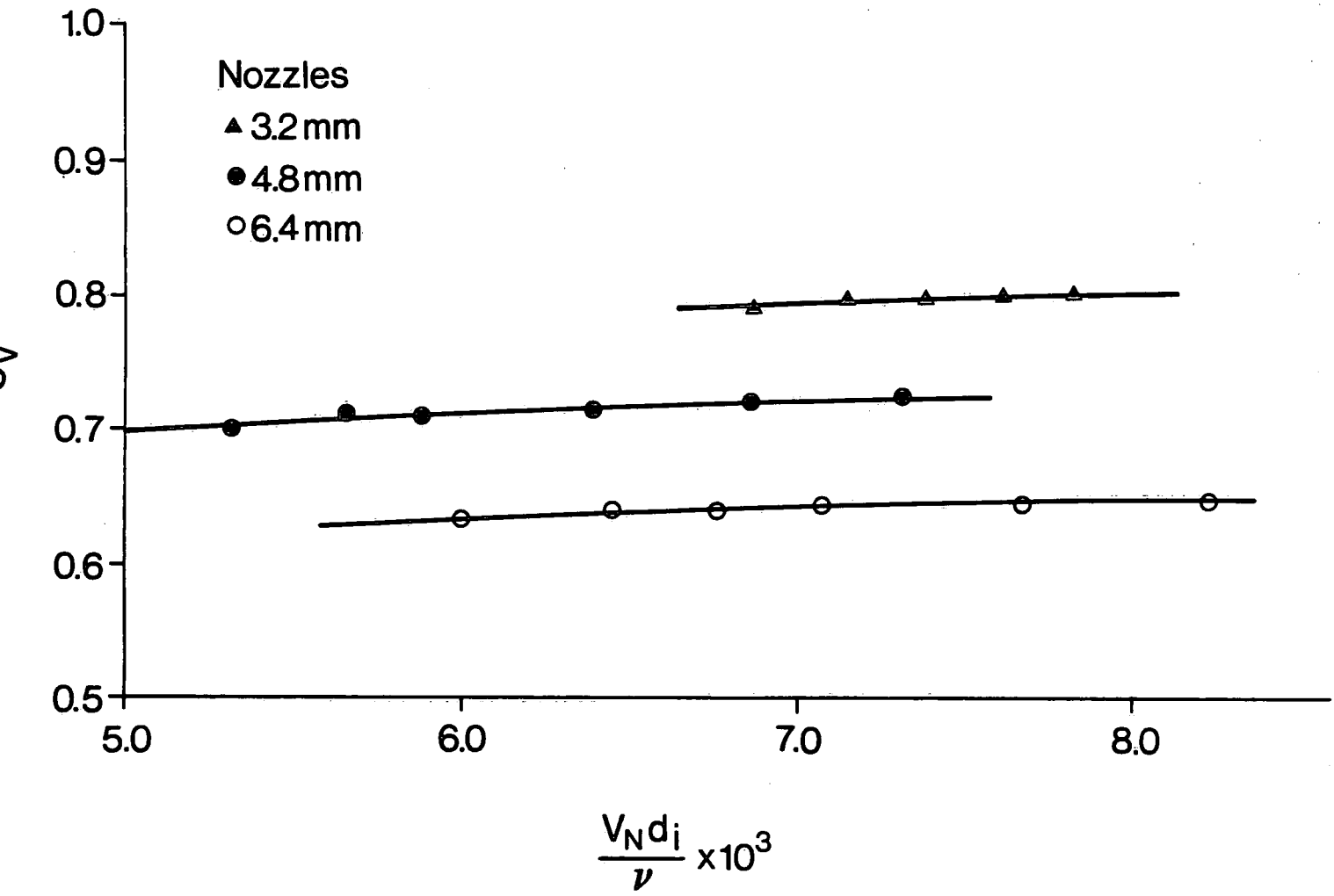

Figure 7 Effect of Reynolds Number on nozzle performance. (Engel, Zrymiak, 1989)

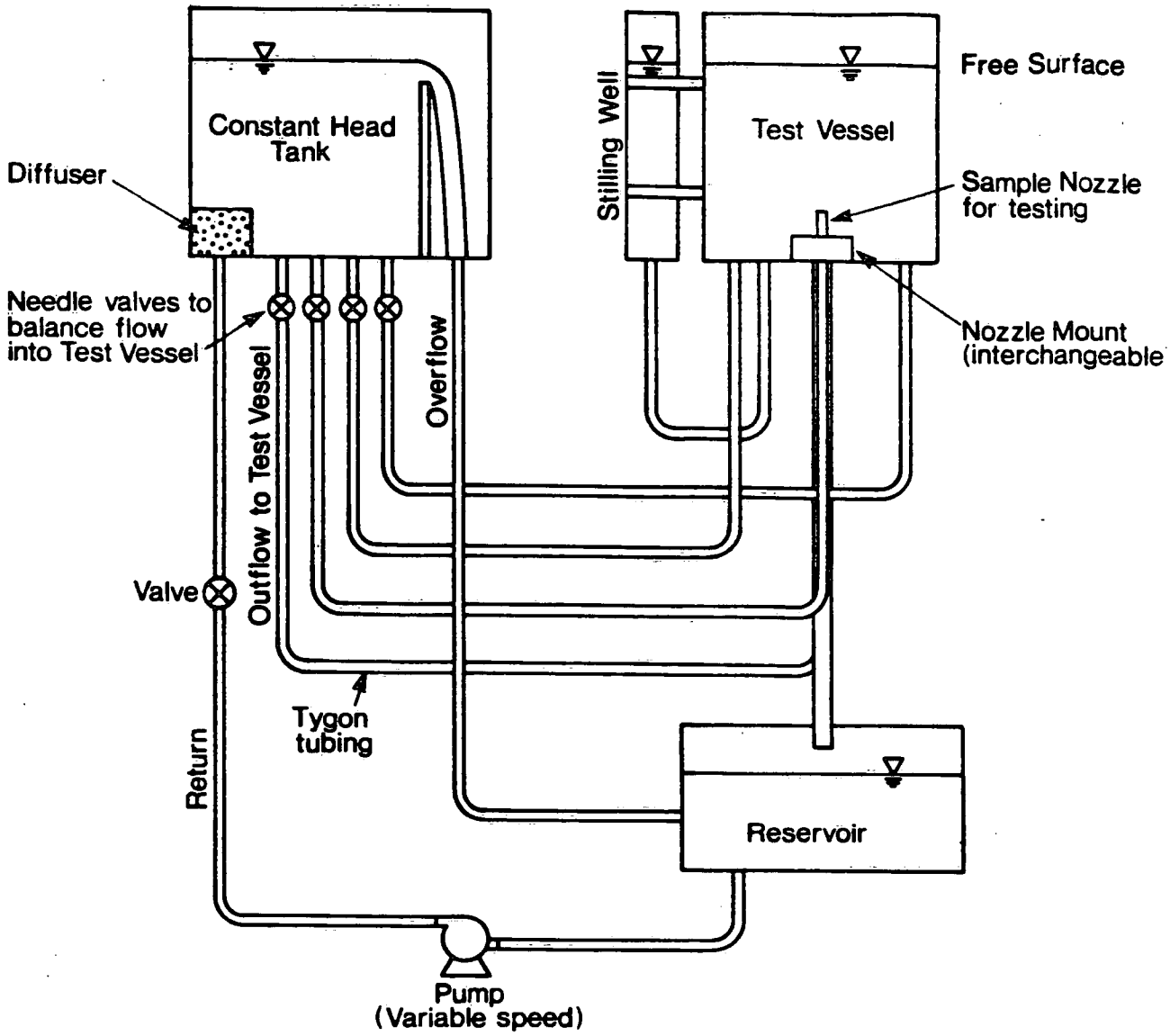

Figure 8 Schematic of static head test facility

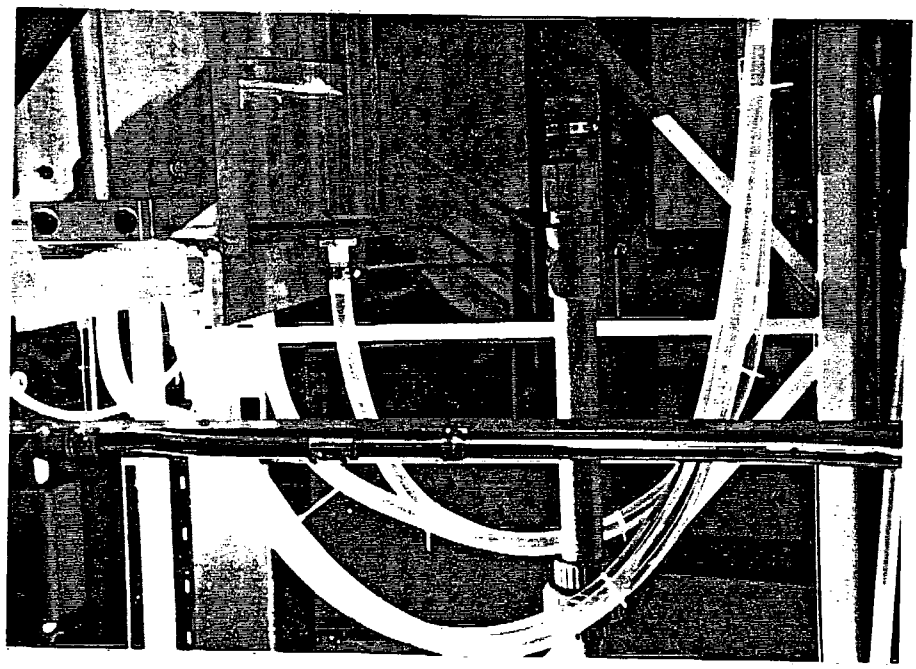

a) Connecting hoses from constant head tank to test chamber.

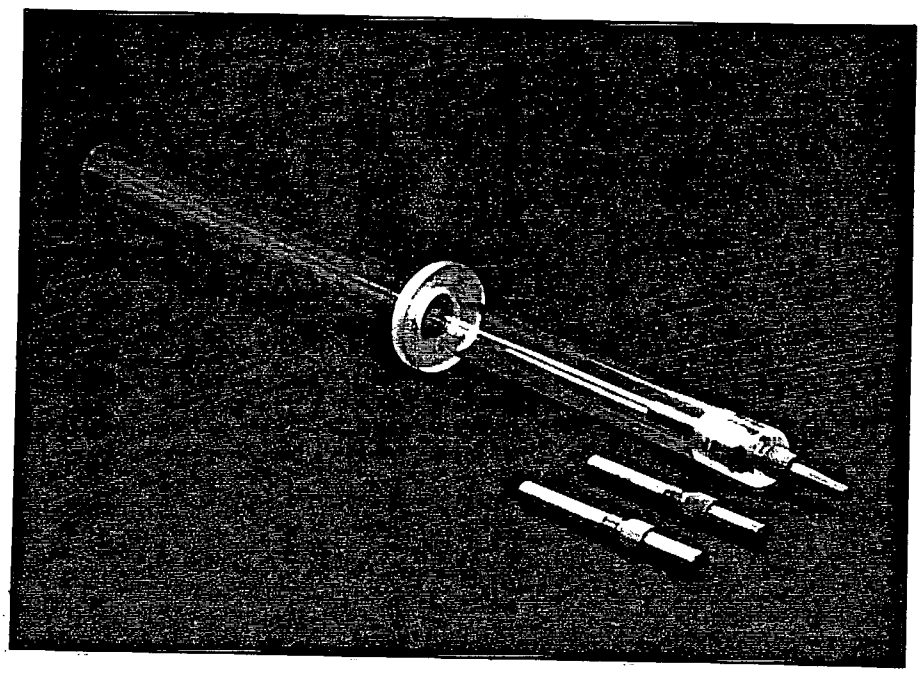

b) Nozzle mount with nozzle

Figure 9 Main flow conduits for test facility

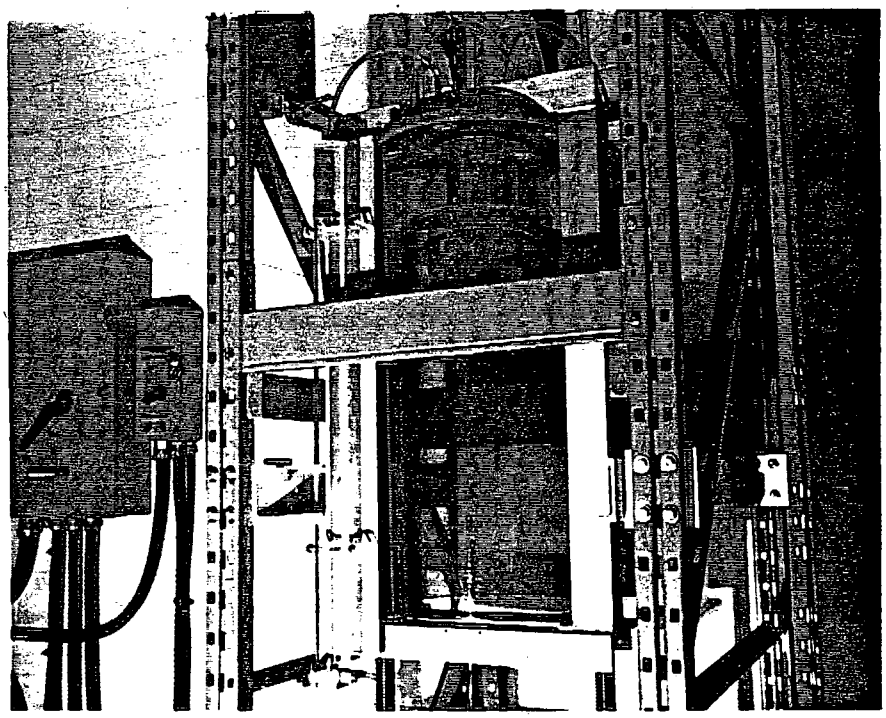

Figure 10 Test chamber and traversing frame

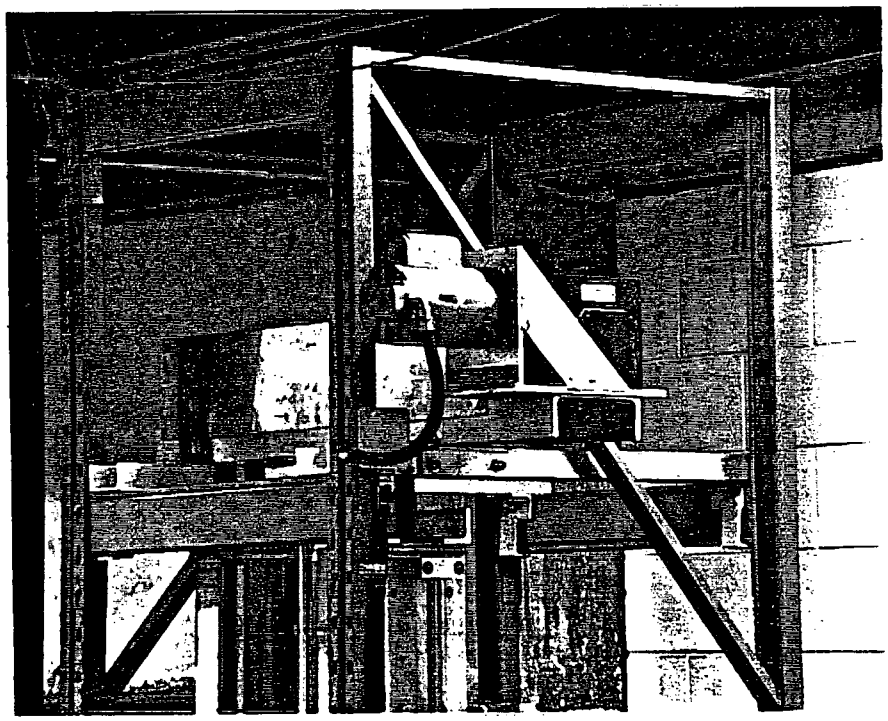

Figure 11 Synchronized drive for test chamber traversing frame

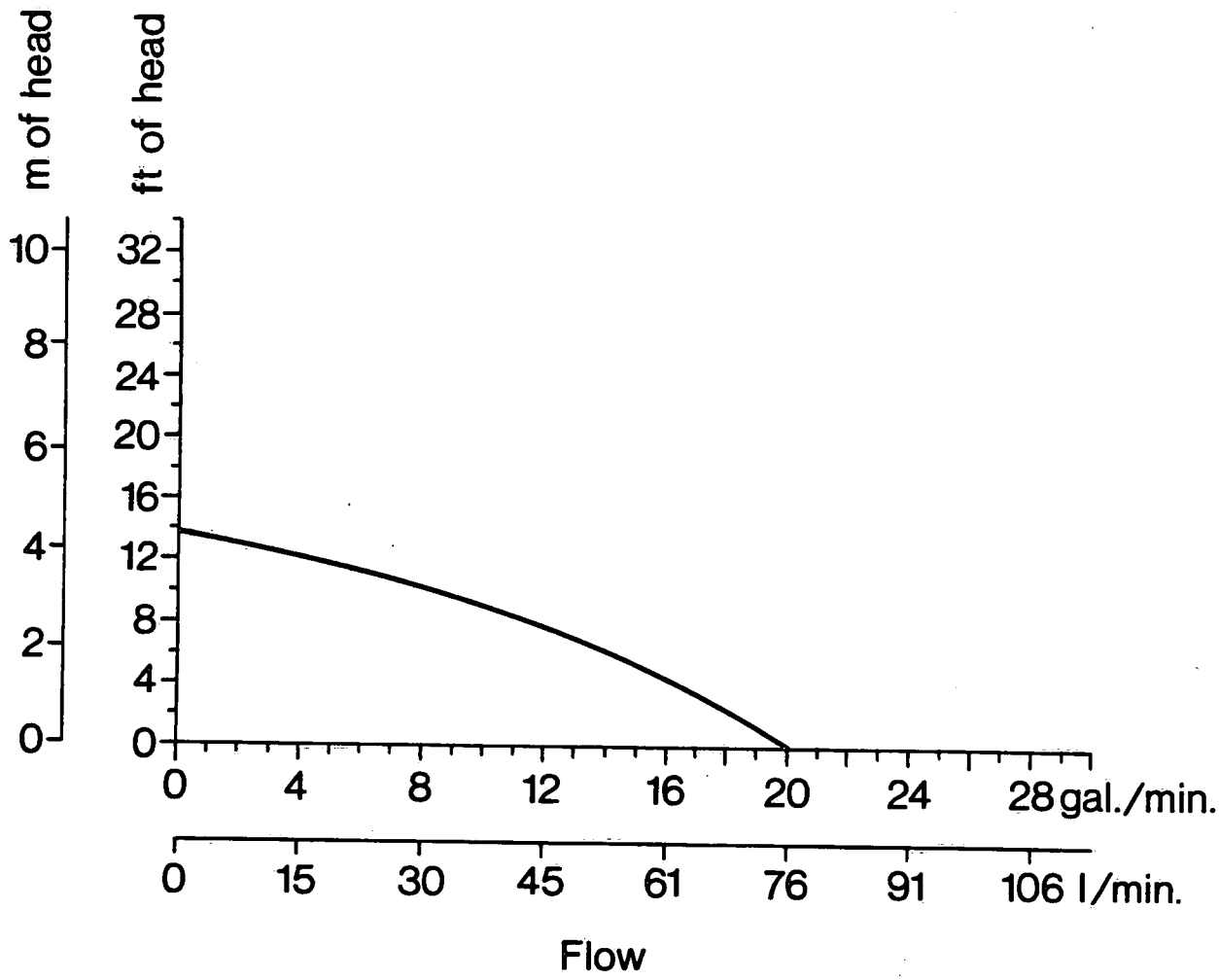

Figure 12 Performance curve for water supply pump

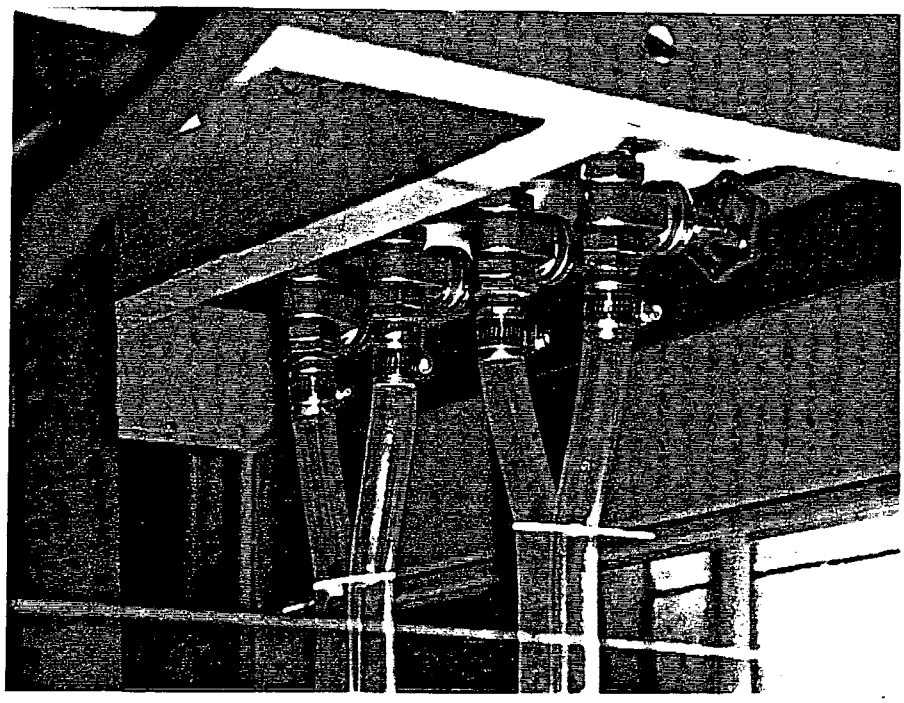

Figure 13 Connection of test chamber water supply hoses to constant head tank.

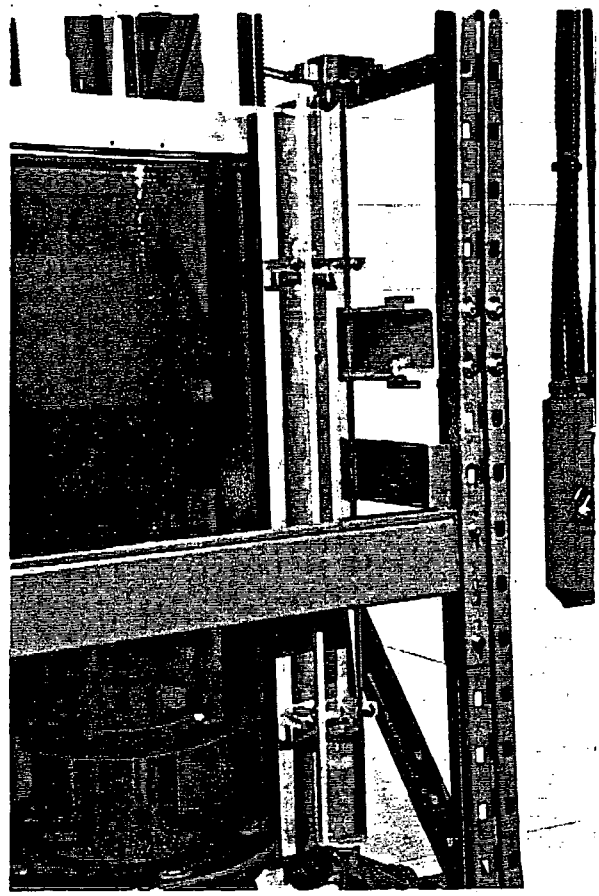

Figure 14 Test chamber stilling well

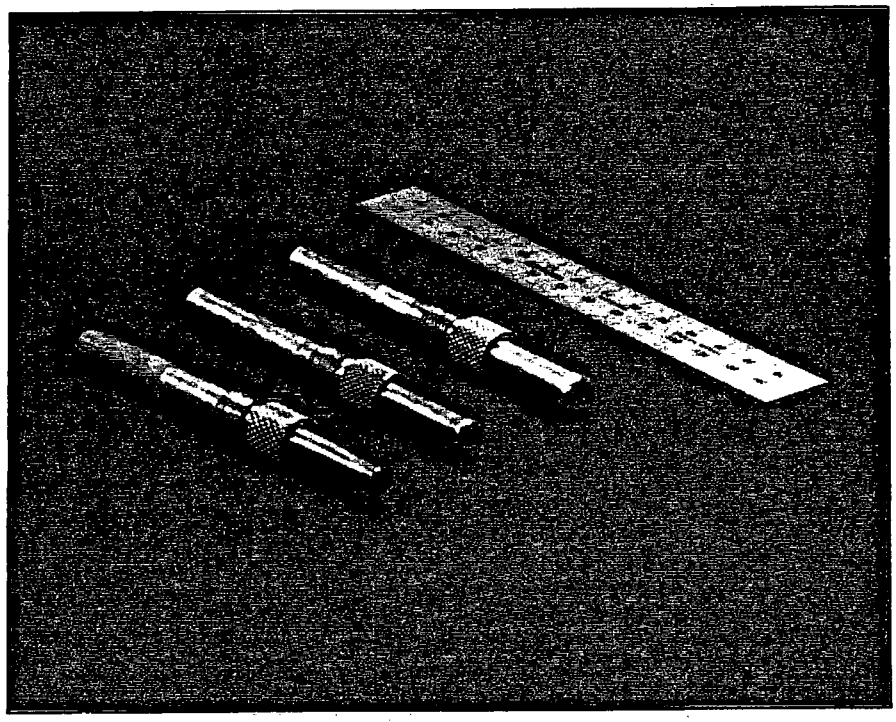

Figure 15 Brass test nozzles

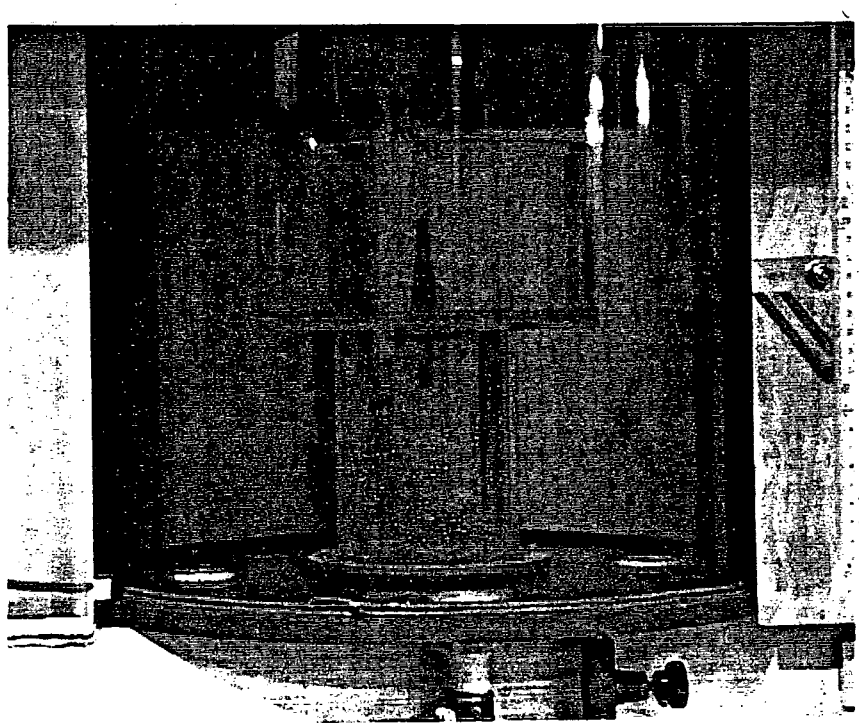

Figure 16 Nozzle and nozzlemount in test position.

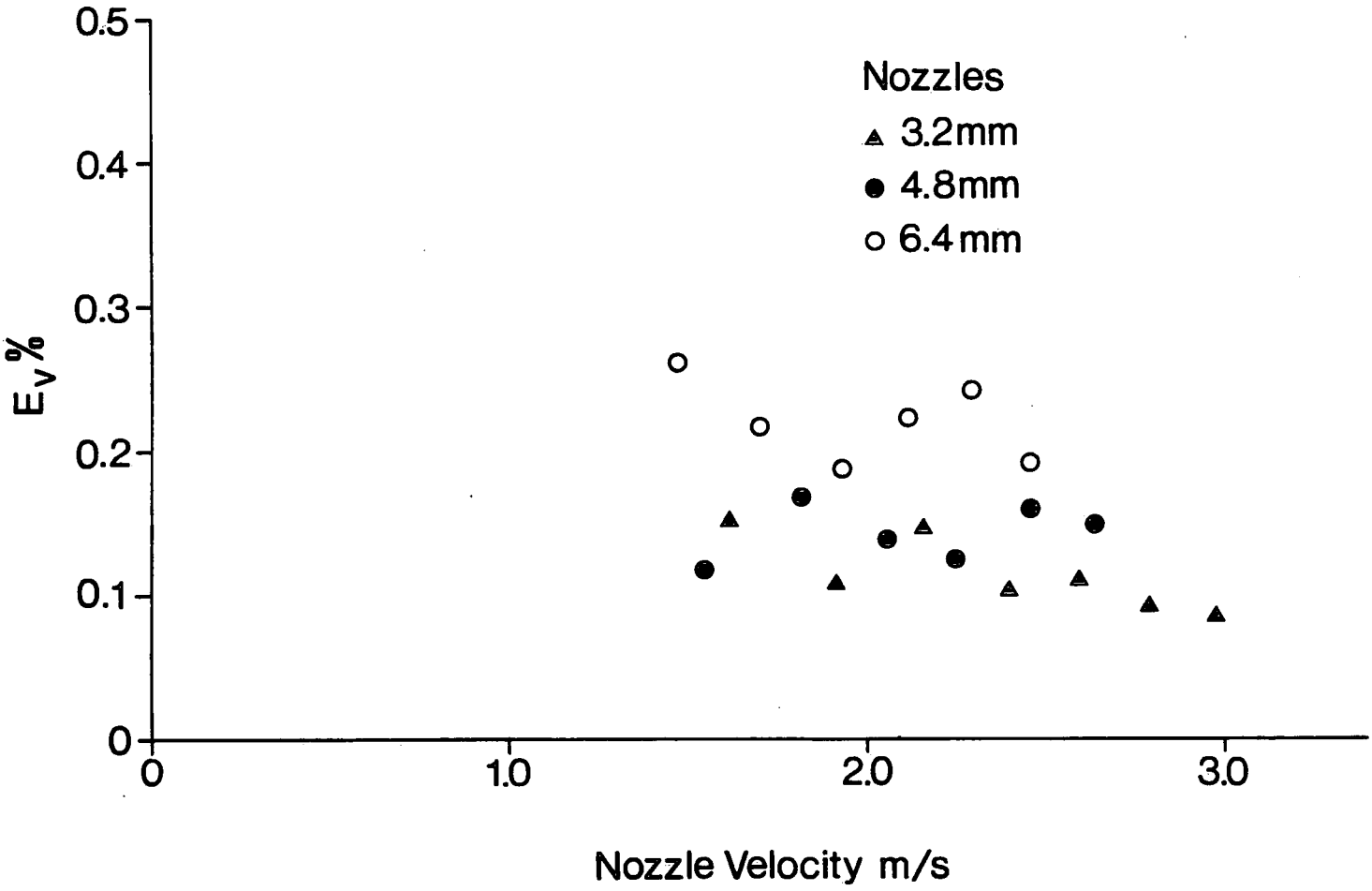

Figure 17 Variability at 95% confidence level in determining V_n

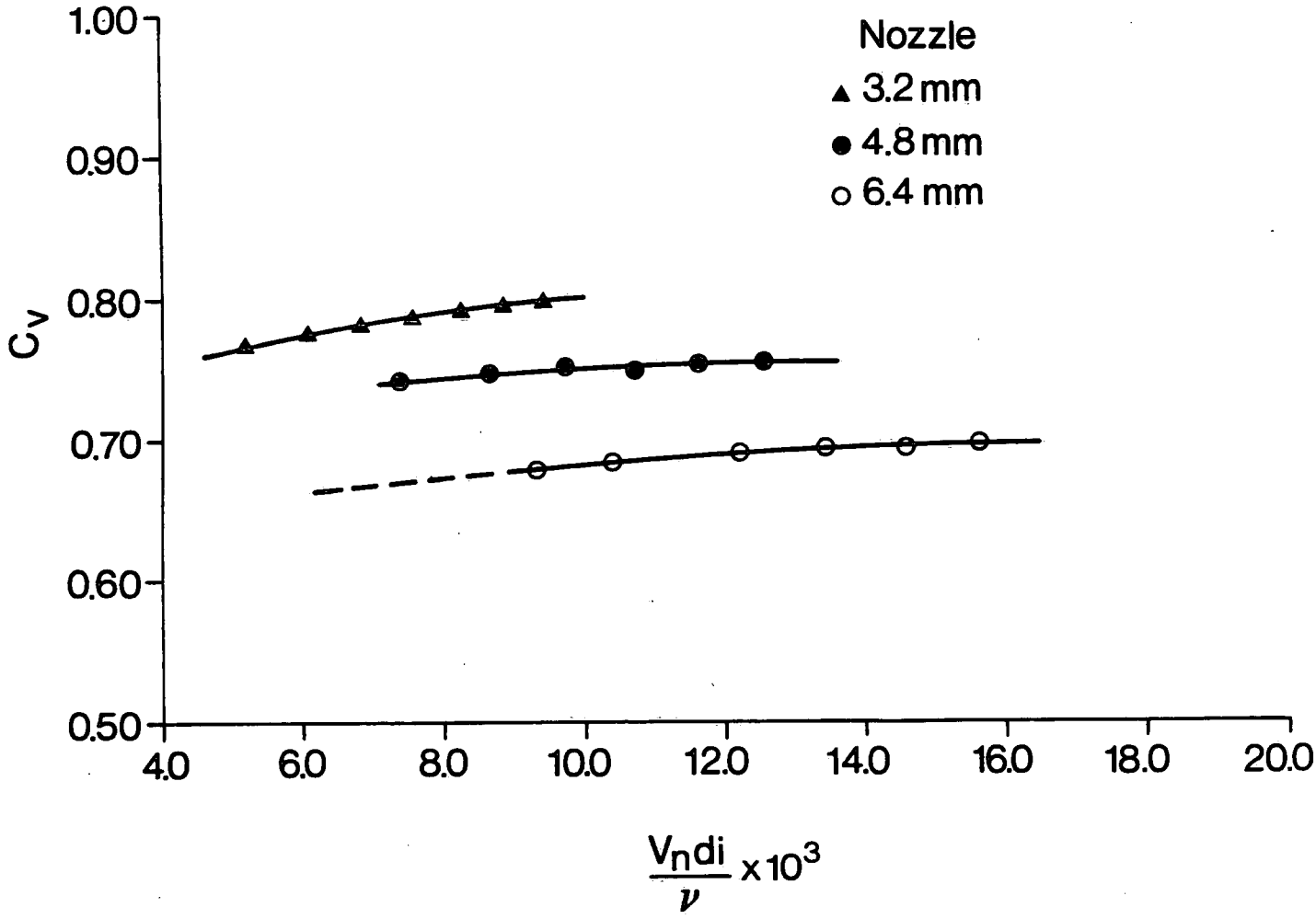

Figure 18 C_V vs. Reynolds Number for test results